Electronic Supporting Materials

ARTICLE

New nanocomposites for SERS studies of living cells and mitochondria

Received 00th January 20xx,
Accepted 00th January 20xx

DOI: 10.1039/x0xx00000x

www.rsc.org/

A. S. Sarycheva[a], N. A. Brazhe,[b] A. A. Baizhumanov,[b] E. I. Nikelshparg,[b] A. A. Semenova,[a] A. V. Garshev[a], A. E. Baranchikov[c], V. K. Ivanov[a,c], G. V.Maksimov,[b] O. Sosnovtseva,[d] and E. A. Goodilin*[,a,c]

A great enhancement of Raman scattering (SERS) from heme - containing submembrane molecules inside intact erythrocytes and functional mitochondria is demonstrated for the first time using silver – silica beads prepared by a new method of aerosol pyrolysis with aqueous diamminesilver (I) hydroxide as a unique source of plasmonic nanoparticles for either the SiO_2 microsheres or graphene oxide flakes and superparamagnetic iron oxides. The recorded SERS spectra revealed a set of characteristic peaks at 750, 1127, 1170, 1371, 1565, 1585 and 1638 cm^{-1} resulting from the normal group vibrations of pyrrol rings, methine bridges and side radicals in the heme molecules. Importantly, the SERS spectra of functional mitochondria were sensitive to the activity of the mitochondrial electron transport chain thus making the method to be a novel label-free approach to monitor the redox state and conformation of cytochromes in their natural cell environment. The developed nanocomposites are highly suitable for the analysis of bilogical objects due to their robust prepared scheme, superior spactial and temporal signal reproducibility preserved for a period of at least one year.

Biocompatible $Ag@SiO_2$ nanocomposites are prepared using a modified aerosol pyrolysis technique with aqueous diamminesilver (I) hydroxide solution as a new source of silver nanoparticles. The silica microspheres can be replaced with other materials if they survive in such alkaline solutions and also undergo no deep decomposition or destruction when heated up to 300 - 800^{0}C (Fig.S1 – S3). Superparamagnetic iron oxides in the form of nanoparticles or flakes of graphene oxide are good candidates for preparation of the nanocomposites.

The colloidal graphene oxide (GO) was formed by the modified Hammers's method of oxidation of graphite powder (TIMCAL TIMREX® KS4, 99.9%). In brief, graphite powder was mixed with sodium nitrate and 98% sulfuric acid inside an ice bath and then $KMnO_4$ was slowly added under magnetic stirring with a control of the temperature of the system to be lower than 70^{o}C. The obtained brownish mixture was accurately diluted with distilled water, then remained $KMnO_4$ and MnO_2 were reduced and dissolved using 3% H_2O_2 while the color of the mixture turned into yellow. The suspension of graphene oxide was left to stay for one night to complete all the reduction processes and then it was centrifuged and washed with distilled water at least three times. Superparamagnetic iron oxide nanoparticles (SPION) of Fe_3O_4 were obtained by a standard reaction of $FeCl_2$ and $FeCl_3$ solutions in an alkaline media followed by washing.

Spraying and decomposition of diammine silver (I) hydroxide solution alone gives purely metallic silver with facetted and sometimes necked spherical particles of different sizes in the range of about 100 - 1000 nm (Fig.S1). The graphen oxide possesses a large amount of different functional groups on the surface being able to reduce silver ions down to silver nuclei and also anchor them. Therefore, TEM images show that the synthesis enables to obtain Ag@GO nanocomposites of different loadings of GO sheets with silver nanoparticles of different sizes. By varying concentration of reagents under 600^{o}C preparation conditions, the silver nanoparticles size of 30 - 40 nm was achieved as optimal for SERS (Fig.S1). Those conditions allowed also to reach different values of specific surface areas of the nanocomposites, namely, 10 m^2/g for the sample with a silver - rich precursor mixture or a much higher area of 99 m^2/g for the excess of graphene oxide.

SPION nanoparticles (Fig.S1 - S3) add magnetic properties to the plasmonic ones of the $Ag@Fe_3O_4$ nanocomposite making them hypothetically interesting for magnetic separation of biological objects combined with an ability of the SERS analysis. The microstructural features of this composite material originate from the fact that aerosol droplets behave as microreactors; thus Fe_3O_4 nanoparticles are self - assembled into submicron hollow microspheres covered with silver nanoparticles.

[a] *Department of Nanomaterials, Faculty of Material Sciences, Moscow State University, Moscow, Leninskie gory 1/3, 119991, Russia.*
[b] *Deparment of Biophysics, Biological Faculty, Moscow State University, Leninskie gory 1/12, Moscow, 119991, Russia.*
[c] *Institute of General and Inorganic Chemistry of Russian Academy of Sciences, Leninsky Ave., Moscow, 119992, Russia.*
[d] *Department of Biomedical Sciences, Faculty of Medical and Health Sciences, Copenhagen University, Blegdamsvej 3, Copenhagen, DK-2200, Denmark*
* - corresponding author, goodilin@yandex.ru, fax +7 (495) 939 09 98.

Electronic Supporting Materials

ARTICLE

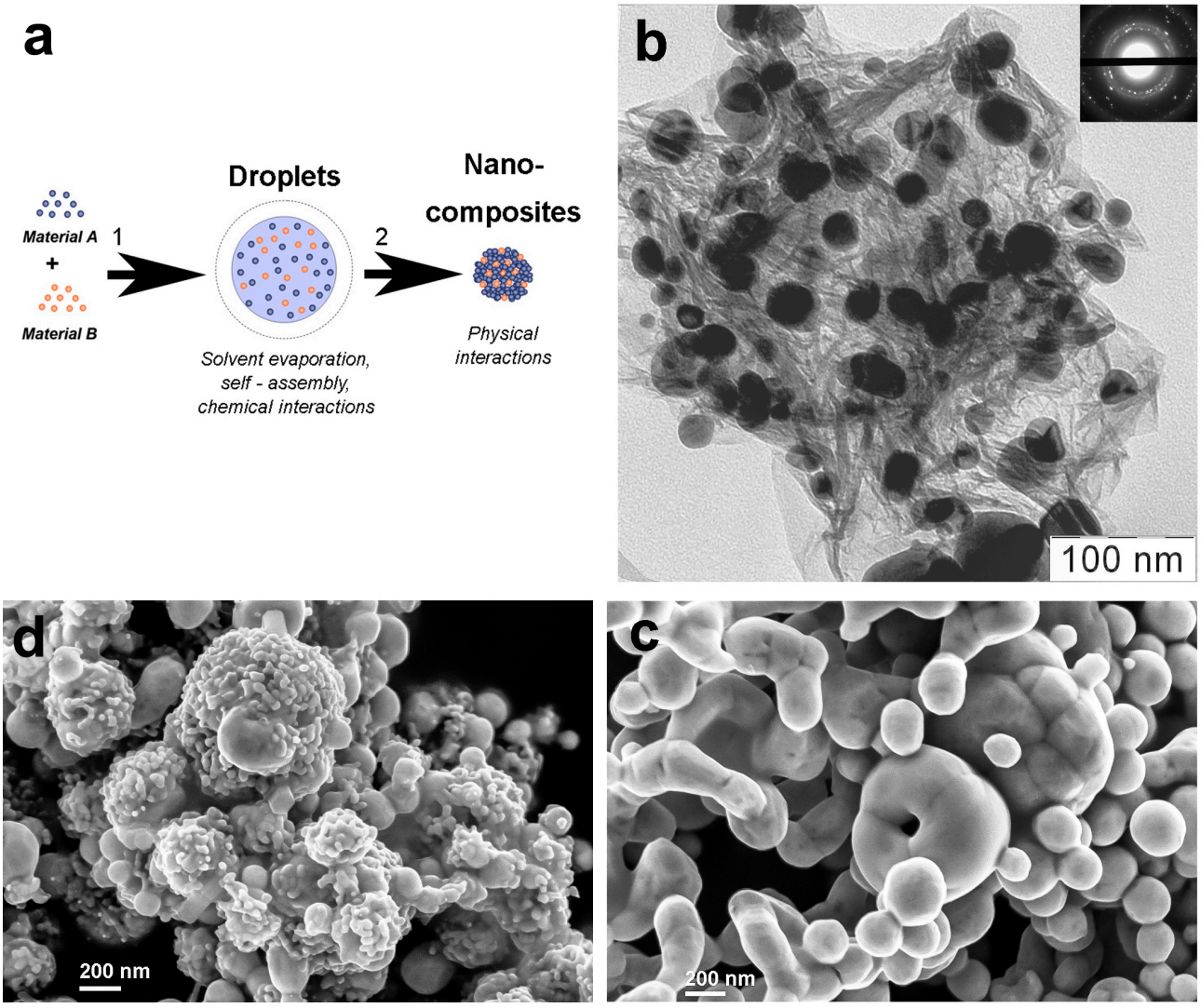

Fig.S1. Polyfunctional colloidosomes / nanocomposites with different core materials prepared by aerosol pyrolysis at 600^{0}C of suspensions containing diamminsilver (I) hydroxide. a. the process scheme, b. application of graphene oxide as a component of the spraying suspension, c - spraying pure solution of diamminsilver (I) hydroxide without solid phases added, d - addition of SPION (Fe_3O_4 magnetic nanoparticles) in the suspension.

Table S1. Summary of optical characteristics of the prepared nanocomposites (see also Fig.S4)

Sample	Pyrolisis temperature, ^{o}C	Silver particle size, nm	UV - vis absorption, nm	Raman bands, cm^{-1}	SERS threshold, M (Rh6G)
Ag	600-600	150 - 3000	435 - 450	-	10^{-7}
Ag@SiO_2	600-800	20 - 80	420 - 450	Smoothed background	10^{-10}
Ag@Fe_3O_4	600-800	90 - 500	400 - 600, broad peak	1300, 1600, broad peaks	10^{-6}
Ag@GO	600	20 - 60	450 - 700, broad peaks	1200 - 1700, D-, G- modes of graphene	10^{-6}

Electronic Supporting Materials

ARTICLE

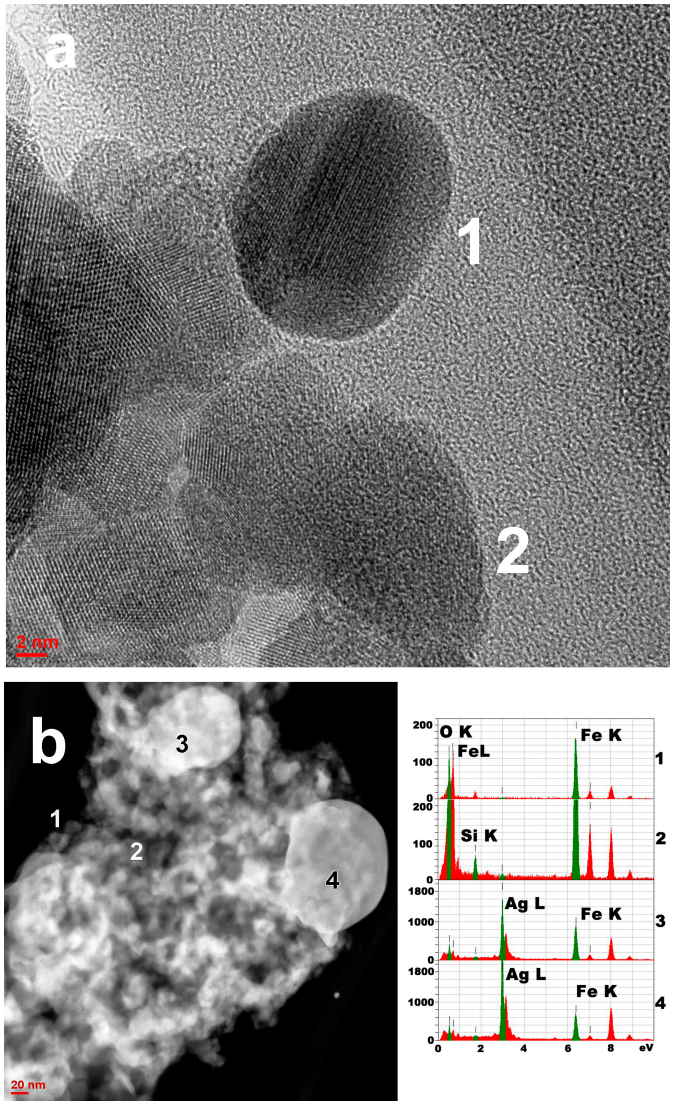

Fig.S2. TEM view of the magnetic colloidosomes with plasmonic silver nanoparticles, Ag@Fe_3O_4. a. HREM image of the nanocomposite, 1 - silver nanoparticle, 2 - Fe_3O_4 component nanoparticles, b. STEM image with local chemical analysis (on the right), 1, 2 points - mostly iron and oxygen atoms, 3, 4 - mostly silver atoms.

Preparation of SERS - active nanocomposites (Table S1) using the proposed carriers of silver nanoparticles results in quite different optical properties which allow to differentiate the materials in terms of their practical applications, particularly, in the light of the present study. Spraying of pure diamminesilver (I) hydroxide solution leads to a material with moderate SERS enhancement coefficients (Fig.S4).

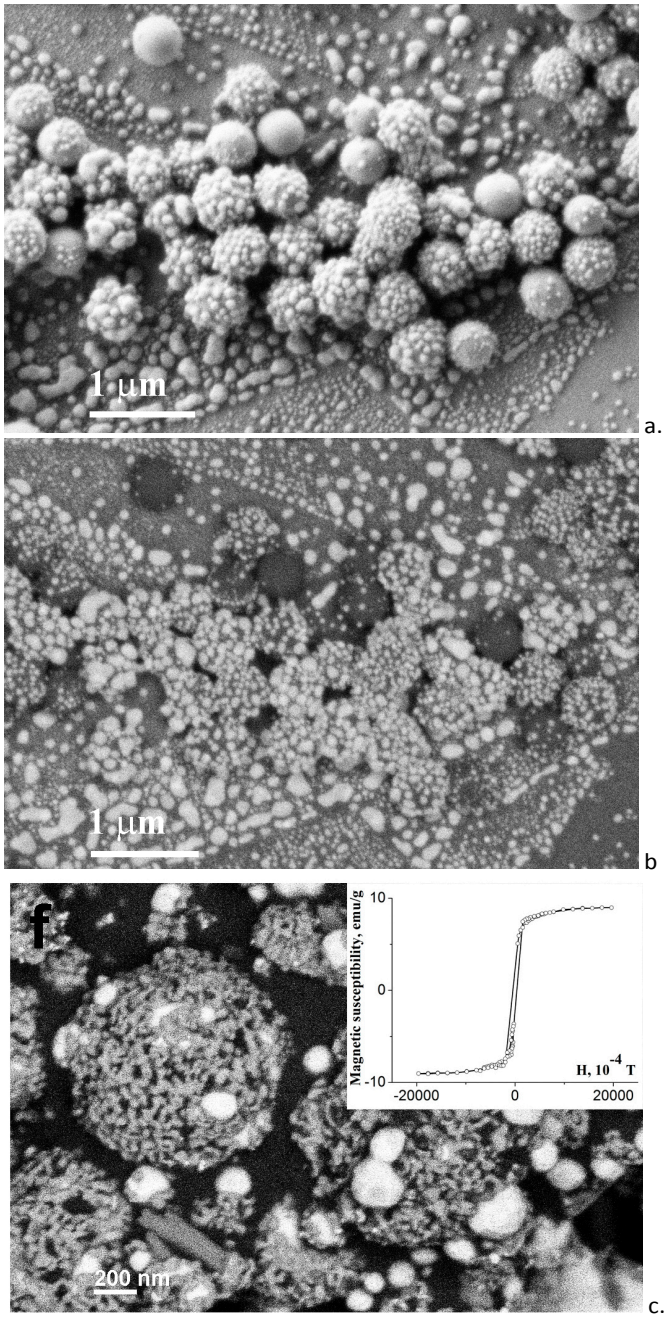

Fig.S3. Variation of constructing particles and spraying conditions of their suspensions in aqueous $[Ag(NH_3)_2]OH$. a,b. spraying of a stream of aerosol droplets of Stober silica microspheres in diammine silver (I) hydroxide solution onto warm (300^{0}C) glass substrates, BSE and SEI SEM modes, c. addition of SPION (Fe_3O_4 magnetic nanoparticles) into a suspension based on $[Ag(NH_3)_2]OH$, BSE mode, the inset shows a narrow magnetic hysteresis loop for this type of as - prepared nanocomposite.

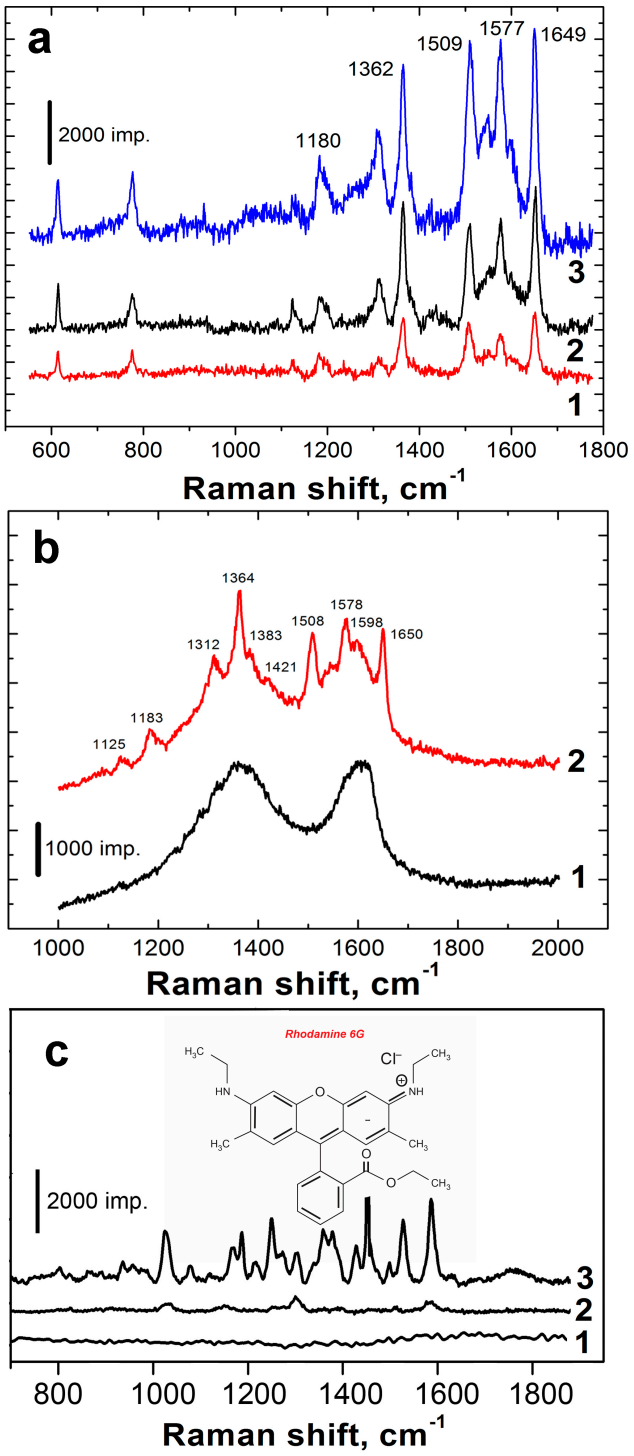

Fig.S4. SERS spectra of a model Rhodamine 6G dye using different nanocomposites produced by aerosol spray pyrolysis with aqueous diammine silver (I) hydroxide (514 nm lasers, excitation power 1.5 mW; objective x5, NA 0.15). a. pure silver powders, 10^{-7} M Rh6G, 1 - 10s registration time, 1% power, 2 - 30s registration time, 1% power, 3 - 10s registration time, 5% power, b. silver – graphene oxide nanocomposite (1 - Rh6G of 10^{-8}M, 2 - Rh6G of 10^{-6}M), c. $Ag@SiO_2$ colloidosomes: $Ag@SiO_2$ materials themselves ("1"), Rh6G of 10^{-10}M ("2") and the same of 10^{-8}M concentration ("3").

Moreover such powder contains purely metallic, concentrated silver which increases consumption of this noble metal for the SERS analysis. The $Ag@Fe_3O_4$ nanocomposites show even a smaller detection thresholds of the Rhodamine 6G dye (Table S1). The main problem of the Ag@GO materials is the presence of distinct peaks of D – and G- modes of graphere and their positions are unfortunately coincided with the most informative bands of heme – like fragments (Fig.S4). This makes it difficult or inappropriate to apply Ag, $Ag@Fe_3O_4$ and Ag@GO nanomaterials for a study of the target biomolecules.

Table S2. EDX composition (in %) of $Ag@SiO_2$ nanocomposites in different random areas of measurements

Element	Area 1	Area 2	Area 3	Area 4	Area 5
O	58	55	52	60	62
Si	27	24	27	26	24
Ag	15	21	21	14	14

Aerosol deposition of a suspension of silica microspheres in aqueous diammine silver (I) hydroxide onto warm substrates (Fig.S3) produces a mixture of silica - silver colloidosomes organized into walls and also aggregates of silver nanoparticles formed directly from $[Ag(NH_3)_2]OH$. The silver nanoparticle aggregates deposit onto silica microspheres completely if they are the only solid phase in the aerosol droplets in usual experiments described in the main article (Table S2). Such prepared colloidosomes demonstrate a different SERS enhancement for a model Rhodamine 6G dye (Fig.S4). Main vibration modes of cytochrome *c* are presented in Table S3.

Table S3. Assignment of the main peaks in SERS spectra of purified cytochrome *c* (based on Refs.[1-7]).

Isolated cytochrome *c*		**Vibration symmetry**	**Sensitivity**
Oxidized	**Reduced**		
1638	1608	B1g	Spin state of heme Fe, diameter of porphyrin ring
1585	1549	A2g	Spin state of heme Fe, diameter of porphyrin ring
1569		B1g	Spin and Redox states of heme Fe
1403	1400	B2g	Redox state of heme Fe
1373	1363	A1g	Redox state of Fe
1317	1316		Redox state of heme Fe
1172	1172	B2g	Redox state of heme Fe
1130	1130	B1g	The potential of the internal mitochondrial membrane
758	758	B1g	Redox state of heme Fe
	690		Redox state of heme Fe

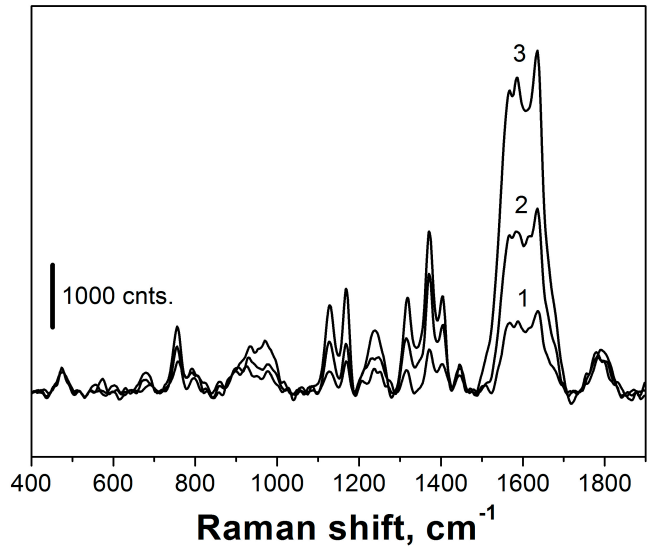

Fig.S5. SERS spectra of mitochondria with no addition of either substrates for the ATP synthesis or electron donors for ETC (1), with an addition of substrates for the complex I and ATP synthesis (ADP (0.1 mM), $MgCl_2$ (2 mM), pyruvate (2 mM), malate 2 mM) (2) followed by an addition of succinate (5 mM) as a donor of electrons for the complex II (3).

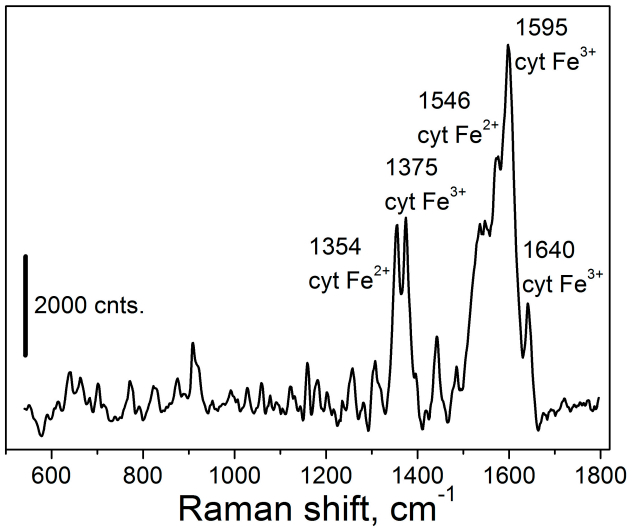

Fig.S6. SERS spectrum of intracellular mitochondria in rat peritoneal macrophages incubated with SiO_2@Ag colloidosomes for 3 h. The "cyt" notation means peaks of cytochromes in a reduced (Fe^{2+}) or oxidized (Fe^{3+}) states.

Consequent additions of electron donors for the complex I of mitochondria (malate and pyruvate) and substrates for the ATP synthesis (ADP and $MgCl_2$) and, afterwards, a succinate - electron donor for the complex II result in a gradual increase of the intensity of SERS spectra of functional mitochondria (Fig.S5).

In order to perform a perspective study whether the produced Ag@SiO_2 nanostructures can be used to study intracellular mitochondria, we used rat peritoneal macrophages incubated with the Ag@SiO_2 colloidosomes for 3 h. After such an incubation, the macrophages were fixed with glutaraldehyde to perform Raman investigations (Fig.S6).

Isolation of macrophages was done as described in ref[8]. Briefly, macrophages were removed from the peritoneal cavity of male Wistar outbred rats, according to a standard procedure with modifications. Suspension of peritoneal cells was layered over 30% Ficoll DL-400 (Sigma, USA) in PBS buffer (145 mM NaCl, 2,7 mM KCl, 2 mM KH_2PO_4 , 4.6 mM Na_2HPO_4, 1 mg BSA per ml, 5 mM D-glucose, 1 mM $CaCl_2$, pH 7,4). Macrophages were separated by centrifugation at 3000 g for 30 min at 4°C. The cell fraction was carefully collected using Pasteur pipette at the interface between the buffer and Ficoll. Then the cell fraction was transferred to a 10 ml red cell lysing solution (201 mM NH_4Cl, 12.5 mM $KHCO_3$, 1.6 mM EDTA) and the suspension was centrifuged at 500 g for 5 min at 4°C. The resulting supernatant was decanted, then the purified macrophages were suspended in a PBS buffer (pH 7.4). Experimental samples contained adherent cells only.

To record SERS spectra, we used the 514 nm laser with its power of 0.1 mW, 100^x objective, NA 0.9. The spectra were recorded from various spots inside macrophages containing either visually observed Ag@SiO_2 particles or no particles. We did not observe any defined peaks in the regions without nanoparticles, however, we recorded SERS spectra in several places in cytoplasm of macrophages with Ag@SiO_2 demonstrating peaks of both reduced and oxidized cytochrome c (Fig.S6). However, this result seems to be irreproducible and even quite surprising since Ag@SiO_2 particles are endocytosized and therefore they are surrounded by an additional 10 nm thick membrane layer. There is only a very small probability that intracellular mitochondria would get closely enough to such endocytotic vesicles. Even in such a lucky case, the distance between the Ag@SiO_2 particles and cytochrome c in the mitochondria will be more than 17 nm (10 nm of the vesicle membrane + 7 nm of the outer mitochondrial membrane) and thus Raman scattering can be enhanced only of those cytochrome c that come close to outer mitochondrial membrane. In the future, we will perform a more detailed study on the enhancement of Raman scattering of cytochrome c from mitochondria inside living cells.

References

1. F. Adar, M. Erecinska, *FEBS Lett.,* 1977, **80**, 195—200.
2. S. Berezhna, H. Wohlrab, P. M. Champion, *Biochemistry,* 2003, **42**, 6149—6158.
3. M. Ogawa, et al., *Biochem. Biophys. Res. Commun.,* 2009, **382***,* 370—374.
4. N. A. Brazhe, et al., *PLoS One*, 2012, **7**, e41990.
5. N. A. Brazhe, et al., *PLoS One*, 2013, **8**, e70488.
6. M. Okada, et al. *Proc. Nat. Acad. Sci. USA,* 2012, **109**, 28—32.
7. N. A. Brazhe, et al., *Sci. Rep.*, 2015, **5** (13793), DOI: 10.1038/srep13793
8. A. I. Yusipovich, A. A. Bayzhumanov, T. A. Kazakova, A. A. Cherkashin, T. R. Kamaletdinova, S. K. Pirutin, N. O. Rozhkova, G. V. Maksimov., International Journal of Biology; Vol. 7, No. 4; 2015